

Short communication

A graphite-granule membrane-less tubular air-cathode microbial fuel cell for power generation under continuously operational conditions

Shijie You^a, Qingliang Zhao^{a,*}, Jinna Zhang^a, Junqiu Jiang^a,
Chunli Wan^a, Maoan Du^a, Shiqi Zhao^b

^a State Key Laboratory of Urban Water Resources and Environments (SKLUWRE), School of Municipal and Environmental Engineering, Harbin Institute of Technology, Harbin 150090, China

^b College of Ship Engineering Institute, Harbin Engineering University, Harbin 150001, China

Received 9 June 2007; received in revised form 23 July 2007; accepted 23 July 2007

Available online 6 August 2007

Abstract

An air-cathode microbial fuel cell (MFC) is an efficient and sustainable MFC configuration for recovering electrical energy from organic substances. In this paper, we developed a graphite-granule anode, tubular air-cathode MFC (GTMFC) capable of continuous electricity generation from glucose-based substrates. This GTMFC produced a maximum volumetric power of 50.2 W m^{-3} at current density of 216 A m^{-2} ($R_{\text{EX}} = 22 \Omega$). Electrochemistry impedance spectroscopy (EIS) measurements demonstrated an overall internal resistance of 27Ω , consisting of ohmic resistance of $R_{\text{ohm}} = 13.8 \Omega$ (51.1%), a charge-transfer resistance of $R_c = 6.1 \Omega$ (22.6%) and a diffusion resistance of $R_d = 7.2 \Omega$ (26.3%). Power generation with respect to initial chemical oxygen demand (COD) concentration was described well by an exponential saturation model. Recirculation was found to have a significant effect on electrochemical performance at low COD concentrations, while such effect was absent at high COD concentrations. This study suggests a feasible and simple method to reduce internal resistance and improve power generation of sustainable air-cathode MFCs. Crown Copyright © 2007 Published by Elsevier B.V. All rights reserved.

Keywords: Graphite-granule; Membrane; Air-cathode; Microbial fuel cell; Volumetric power; Internal resistance

1. Introduction

Efficiently making use of biological processes to recover useful energy from organic wastes is always a goal for the wastewater treatment industry. At present, microbial fuel cells (MFCs) are considered to be a very popular and promising bio-electrochemical power source for directly recovering electrical energy from carbohydrates as well as organics in wastewater. Several bacteria, including many *Geobacter* species [1], *Shewanella putrefaciens* [2], *Rhodospirillum rubrum* [3], *Clostridium butyricum* [4] and *Aeromonas hydrophila* [5] have been known capable of oxidizing organic substances with the electrode serving as the electron acceptor to produce electrical current. In summary, electricity production in an MFC principally comprises four steps: (i) anodic bio-catalyzed oxidation of organic matter; (ii) physical electron transfer to the

electrode via microbial self-produced chemical shuttles [6], biologically produced nanowires [7], or chemically active redox enzymes [8] with simultaneous proton transport in solution from the anode into the cathode; (iii) electron conduction across the external circuit; and (iv) cathodic reduction of oxidants.

In MFCs, catholytes such as potassium ferricyanide [9–11] or potassium permanganate [12] can be used for optimizing cathodic reactions. These liquid-state electron acceptors, however, may be impractical and unsustainable for practical uses due to a requirement of regeneration of the chemicals. Alternatively, an air-cathode MFC allows use of oxygen freely available in the air as the electron acceptor, considerably improving the process sustainability and decreasing the operational costs of the cell [13]. Previously reported air-cathode MFCs have used a single tube as the main body with the anode and cathode placed on opposite sides of the reactor [13–16]. Such a design pattern may be problematic for scale up of the system because close electrode spacing can lower the overall capacity of the system. On the other hand, power generated

* Corresponding author. Tel.: +86 451 86283017; fax: +86 451 86282100.
E-mail address: qlzhao@hit.edu.cn (Q. Zhao).

with air-cathode MFCs is usually lower than that produced by liquid-chemical catholyte MFCs. Thus, there is a need to further improve the electrochemical performance of air-cathode MFCs.

Internal resistance is one of the most significant limitations to increasing power generation in MFCs [17]. Under working conditions, internal resistance in a fuel cell can be classified as charge-transfer resistance, ohmic resistance, and mass-transfer resistance. Ohmic resistance is generally considered to be the dominant component, and its magnitude depends on MFC configuration rather than the specific bacteria [18]. Therefore, constructing an air-cathode MFC with low internal resistance is of great importance. It has been shown that power can be increased in a ferricyanide-cathode MFC by using a tubular anode [19,20], a tubular ferricyanide- or permanganate-cathode bushing MFC [12], or by using an MFC open-to-air with a membrane-less cathode [16]. However, there has been no previously reported attempt to increase power by combining a tubular anode and a membrane-less cathode together into one integrated system.

The goals of the present study were to: (i) examine continuous power generation in graphite-granule, membrane-less tubular air-cathode MFC (GTMFC); (ii) evaluate internal resistance using electrochemistry impedance spectroscopy (EIS); and (iii) to investigate the dependence of electrochemical performance on the initial COD concentration and on amount of liquid recirculation.

2. Materials and methods

2.1. MFC construction

The GTMFC was constructed using a 3-cm diameter and 13.5-cm high cylindrical Plexiglas tube (20-mm thick) with the total volume of 95 mL. A conical cover was placed on the top of the cell to collect the effluent stream, and an influent port was placed at the bottom of the reactor for the influent stream. Holes (2.0 mm in diameter) were homogeneously drilled through the wall of the anode, resulting in a geometrical surface area of 60 cm² available for proton transport from the anode to the cathode. Anodic carbon granules (Jiangsu province, China) were screened to produce diameters of 3–5 mm (55 m² m⁻³). The wet volume of the anodic zone was 55 mL (net electrochemical volume) and the surface area of the carbon granules was estimated as 31 cm². The granules were connected to the circuit using a graphite rod (diameter 1 cm and length 5 cm) inserted into the packed bed of granules. The cathode was made of a piece of flexible carbon cloth (E-TEK, 30% wet proofing; 10 cm × 10 cm in size; effective area of 90 cm²) tightly bonded around the outside wall of the tube. Fine C/Pt powders (Pt content 20%; E-TEK) were coated onto the inside surface of the cathode at a loading rate of 0.8 mg-Pt cm⁻² perfluorosulfonic acid (Nafion) solution as a binder. The cathode was prepared with a carbon/PTFE layer applied by methods described by Cheng et al. [21]. The graphite rod in the anode and the cathode was connected by copper wires. The schematic of the GTMFC reactor is shown in Fig. 1.

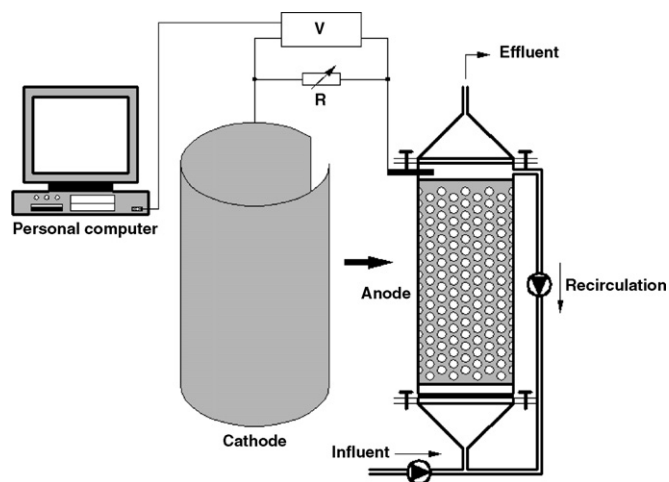


Fig. 1. The schematic of the main structure of the GTMFC.

2.2. Inoculations and operations

The GTMFC was inoculated with anaerobic sludge collected from a thickening tank at the Wenchang wastewater treatment plant in Harbin, China. Prior to being used, anaerobic seed sludge was diluted by distilled water, followed by being filtered through a 0.15-mm pore mesh to remove coarse particles. During the start-up phase, seed sludge with nutrient solution was continuously fed into the MFC. The anodic medium contained (per liter of deionized water): glucose (0.6 g; 600 mg COD L⁻¹), NaHCO₃ (1 g), KCl (0.13 g), NaH₂PO₄ (4.22 g), Na₂HPO₄ (2.75 g), (NH₄)₂SO₄ (0.56 g), MgSO₄·7H₂O (0.2 g), CaCl₂ (15 mg), FeCl₃·6H₂O (1 mg) and MnSO₄·H₂O (20 mg). Trace elements were also added in the solution as previously described [22]. Anolyte was continuously added into the reactor at a fixed flow rate of 0.4 mL min⁻¹, and recirculated from the upper port back to the bottom using two separate peristaltic pumps (type BT100-1Z, China) as shown in Fig. 1. The recirculation ratio (RR) is a ratio of the recirculation flow rate (mL min⁻¹) to the influent flow rate (0.4 mL min⁻¹). All the experiments and tests were conducted at constant environmental temperature (25 °C) and atmosphere pressure (1.013 MPa).

2.3. Calculations and analyses

Voltage generated during experiments for long-term operation were recorded directly every 1 min using a dual-channel voltage collection instrument (12 bit A/D conversion chips, US) and a potentiostat connected to a personal computer via a universal serial bus (USB, Intel) interface. Voltage was converted to power density based on the anodic liquid volume (W m⁻³). Following a stable power generation, the external resistor (R_{EX}) was varied over the range of 1–1000 Ω to obtain a polarization curve. Data for each resistor was collected after the cell exhibited stable power over a minimum period of 5 h.

The observations of bacterial morphologies on the granule carbon (anode) were performed using scanning electron microscope (SEM) (Hitachi, S570; Japan). Before observation, the anodic granules were collected and fixed overnight with

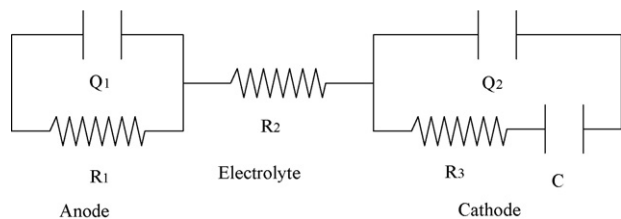


Fig. 2. Equivalent electrical circuit of the GTMFC based on two-time constants. The symbols R and Q represent resistance and capacity elements, in which R_2 is the resistance related to the electrolyte and the numbers 1 and 3 are the representations of the anode and the cathode. C is the double-layer capacitor caused by a gas diffusion layer at the cathode.

paraformaldehyde and glutaraldehyde in buffer solution (0.1 M cacodylate, pH = 7.5; 4 °C), followed by washing and dehydration in water/ethanol solutions. Samples were then coated with Au/Pt before SEM observation.

Internal resistance was characterized using electrochemistry impedance spectrometer (EIS) methods. Scanning was performed after the cell was run at an open-circuit condition for at least 5 h. The impedance measurements were taken from 100 kHz to 10 mHz by applying a sine wave (10 mV rms) on top of the bias potentials with a potentiostat (Parstat 263A, Princeton Applied Research). Data obtained were fitted and simulated by ZSimpWin3.10 software (Echem., US) based on the equivalent electrical circuit illustrated in Fig. 2. The constant phase element (CPE) Q was induced to account for special double layer charging behavior of the porous electrodes. The symbol C represents a double-layer capacitor to account for behavior related to oxygen diffusion from the cathode.

3. Results and discussion

3.1. Anodic bacterial accumulation and stable power generation

During the start-up phase, the anodes in the GTMFC were colonized using seed sludge and a glucose solution (1000 mg COD L⁻¹) in a continuous feed operational mode. As is shown in Fig. 3, there was a gradual increase in voltage across the resistor ($R_{EX} = 50 \Omega$) over an initial time interval of 0–326 h (accumulation period), with the voltage stabilizing at 0.376 V during the next 50 h period (326–375 h). Removing the seed sludge from the inlet flow increased power output slightly, with subsequent electricity production from the glucose-only medium sustained at a stable voltage of 0.384 V for an operational time of about 110 h (375–485 h). This implies that electron-transferring (exoelectrogenic) bacteria colonized the granules and were able to catalyze glucose oxidation and produce current. The morphologies of the bacteria on the anodic carbon granules are seen in SEM images in Fig. 4.

To examine the dependence of the voltage drop and power on current, a polarization curve was obtained as shown in Fig. 5. The open circuit voltage (OCV) of the cell was 0.71 V and the maximum volumetric power of 50.2 W m⁻³ was produced at a current density of 216 A m⁻³ (0.246 V; $R_{EX} = 22 \Omega$). The steep voltage decline at low current density (<50 A m⁻³)

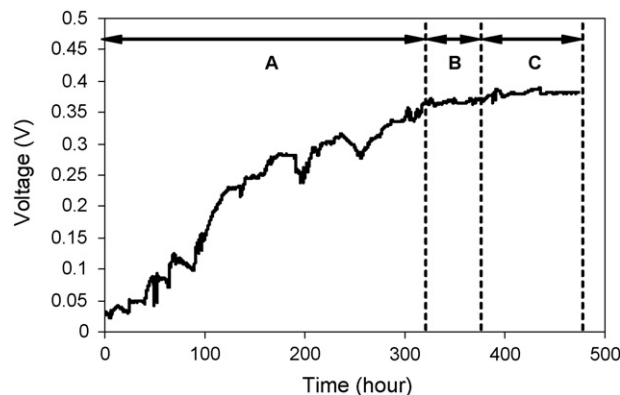


Fig. 3. Continuous voltage generation time profiles for the GTMFC at a fixed resistor of 50 Ω . Note that there are three phases shown in the plot: (A) a lag phase for anodic bacterial accumulation (0–326 h); (B) a phase during which stable voltage output was obtained (326–375 h); and (C) a period of stable voltage generation in the absence of seed sludge (375–485 h).

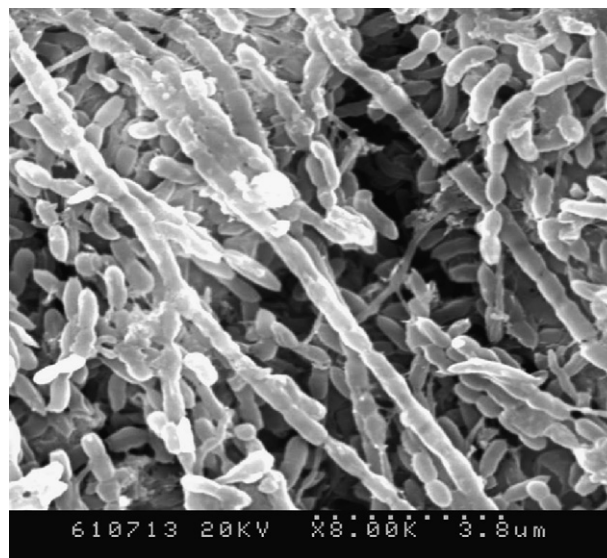


Fig. 4. Morphologies of microorganisms forming on the surface of the anodic granule carbon taken by scanning electron microscope (SEM).

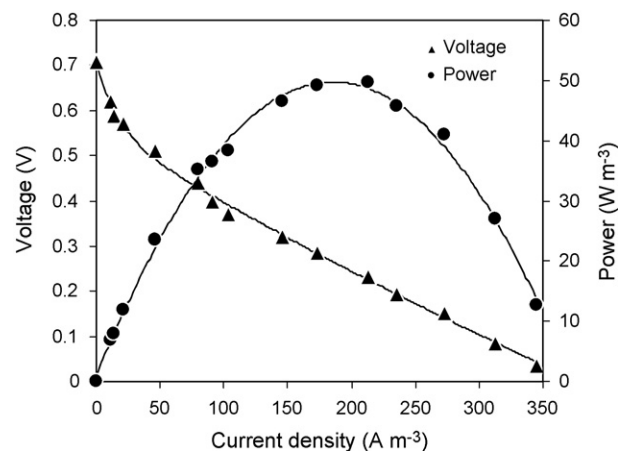


Fig. 5. Volumetric power generation and voltage as function of operating current density in the MFC with glucose (1000 mg COD L⁻¹) as the substrate.

seems likely to have resulted from the resistance associated with activation losses (e.g. a limitation of biological metabolism at the anode and oxygen reduction at the cathode). The maximum power point (MPP) occurs over a linear portion of the $V-I$ curve ($50\text{--}345\text{ A m}^{-3}$), demonstrating an ohmic limitation occurring over a wide region. Although the maximum power of 50.2 W m^{-3} here was at the same level of 51 W m^{-3} obtained by Cheng et al. [16] in an air-cathode MFC, GTMFC appears to be more advantageous because of its ability of holding larger liquid volumes, which is more suitable for large-scale wastewater treatment.

3.2. Electrochemical characterization by impedance spectroscopy

To further study the distribution of internal resistance in the GTMFC, impedance spectroscopy measurements were performed. By fitting the experimental data into an equivalent electrical circuit (Fig. 2) using non-linear least-squares (NLSQ) procedure, we obtained a Nyquist plot (Fig. 6). It was shown that an overall R_{int} of $27\ \Omega$ consisted of an ohmic resistance (R_{ohm}) of $13.8\ \Omega$ (51.1%), a charge-transfer resistance (R_c) of $6.1\ \Omega$ (22.6%) and a diffusion resistance (R_d) of $7.2\ \Omega$ (26.3%), respectively. A large fraction of resistance was in the ohmic resistance, in agreement with the results obtained from the polarization curve. The R_d of 26.3% observed here seems to be much higher than that of 8.5% reported for an internal-cathode MFC [19]. This seems likely to be a consequence of a limitation to proton or oxygen transfer onto the catalyst layer at the air-cathode in the GTMFC. On the other hand, it should also be realized that the $R_{\text{ohm}} = 13.8\ \Omega$ observed here is actually lower than the majority of previously reported values for two-chambered oxygen-cathode MFCs [9,23,24] and a single chambered air-cathode MFC [13,15]. Here the design factors associated with close electrode spacing, removal of membrane, and the use of a flow-through pattern likely account for the lower cell resistance.

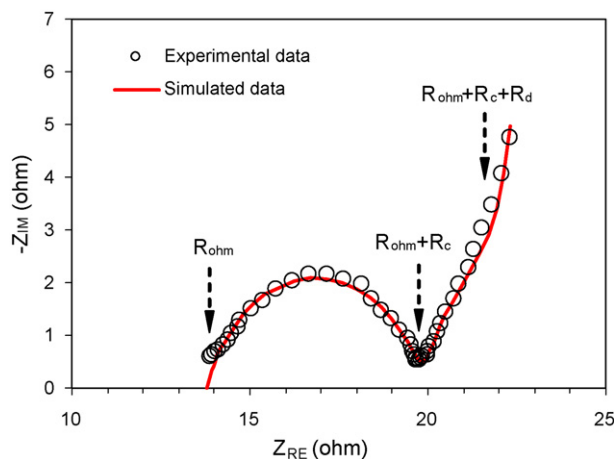


Fig. 6. Nyquist plots of impedance spectra of the GTMFC. Experimental data were obtained and then simulated using the equivalent electrical circuit shown in Fig. 2. The resistance of the cell was characterized as ohmic resistance (R_{ohm}), charge-transfer resistance (R_c) and diffusion resistance (R_d).

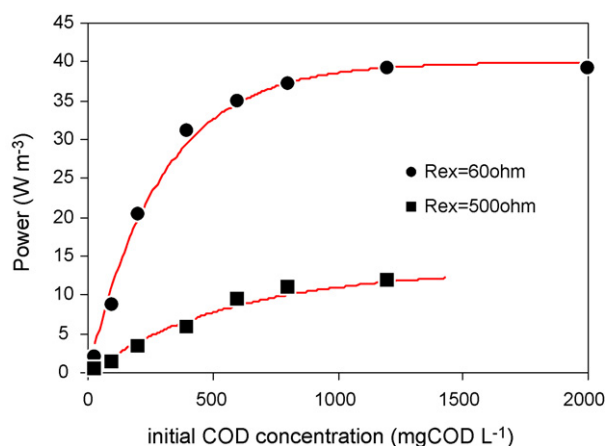


Fig. 7. Power generation as function of initial COD concentration in the analytes with a simulation based on the Teissier equation.

3.3. Effects of initial COD on power generation

The effects of initial COD concentration on power output were studied on day 30. The general dependence of power generation on initial COD concentration appears to be consistent with exponential saturation kinetics (Fig. 7). The Teissier equation [25], $P = P_{\text{max}}(1 - e^{-bC_s})$, was used for a non-linear least-squares fitting of the data in Fig. 7, producing parameters $P_{\text{max}} = 39.94\text{ W m}^{-3}$ and $b = 0.0034\text{ L mg}^{-1}$ for $50\ \Omega$ ($R^2 = 0.995$), and $P_{\text{max}} = 15.47\text{ W m}^{-3}$ and $b = 0.0014\text{ L mg}^{-1}$ for $500\ \Omega$ ($R^2 = 0.989$), respectively. P_{max} is the theoretical volumetric power density (W m^{-3}), b the saturation constant (L mg^{-1}) and C_s the substrate concentration (mg COD L^{-1}). Simulation results indicate that the pattern of power generation corresponded well to that of bacterial growth in the MFC, which may explain why power generation cannot be increased without an upper limitation with increased COD concentration.

3.4. Effects of recirculation on electrochemical behavior of the cell

The effects of recirculation on power production, and the internal resistance distribution at different COD concentrations, were further examined. As shown in Fig. 8 for the MFC operated under high substrate concentration ($2000\text{ mg COD L}^{-1}$), increasing the recirculation ratio (RR) from 0% to 100% only increased volumetric power slightly (7%; $R_{\text{EX}} = 50\ \Omega$). This suggested a minor effect of RR on power yields. At a low substrate concentration (400 mg COD L^{-1}), however, power was substantially increased by a factor of 2 (36.3 W m^{-3} at RR = 100%) compared to that obtained in the absence of recirculation (12.1 W m^{-3} at RR = 0%).

There is a varying dependence of total internal resistance on RR for different substrate concentrations. At $2000\text{ mg COD L}^{-1}$, three resistances (R_{ohm} , R_c and R_d) were essentially constant at for different RRs, indicating a working stability of the cell (Fig. 9A). At 400 mg COD L^{-1} , however, total internal resistance was decreased by 31.3% as the RR was increased from 0 to 100%. This was attributed mainly to the decrease in R_{ohm} (by 41.9%) and R_d (by 25%) as shown in Fig. 9B.

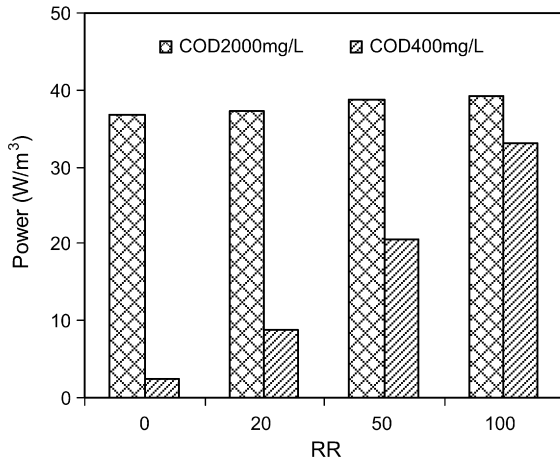


Fig. 8. Effects of recirculation ratio on power generation in the GTMFC ($R_{EX} = 60 \Omega$).

It seems likely that the GTMFC behaves as a completely mixed system with all areas of the anode at the same substrate concentration at high RR, and as a plug flow reactor at low RR such that the substrate was gradually depleted along the height

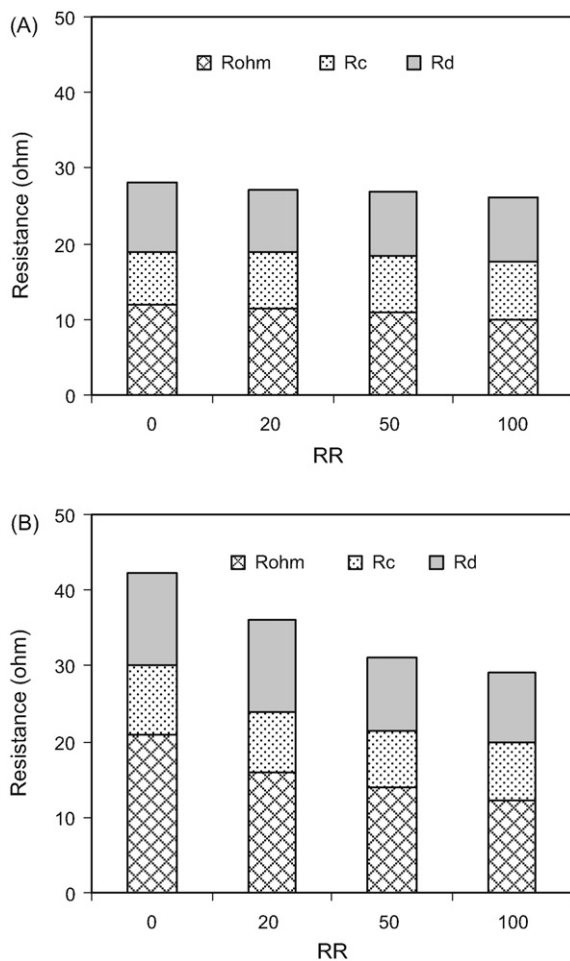


Fig. 9. Dependence of R_{ohm} , R_c and R_d on recirculation ratio at (A) 2000 mg $COD L^{-1}$ and (B) 400 mg $COD L^{-1}$ substrate concentrations. The total resistance (R_t) was the sum of R_{ohm} , R_c and R_d .

of the anode. This may explain the different impacts of RR on electrochemical behavior of the cell at various substrate concentrations. These results imply that the GTMFC would be more effectively operated at high substrate concentration to ensure stable and high levels of power and low operational costs for recirculation.

3.5. Applications of GTMFC in wastewater treatment

Continuous electricity generation from artificial wastewater using a GTMFC was shown here in this proof-of-concept study based on a reactor with an improved air-cathode MFC architecture. This design configuration combines the virtues of both an air-cathode MFC and an up-flow MFC, and it achieves a low internal resistance and a high-level of power output. The maximum volumetric power of $50.2 W m^{-3}$ here is comparable to that of $51 W m^{-3}$ previously obtained using another air-cathode MFC design [16]. However, generating electricity in the GTMFC seems more advantageous than this other design due to the large volumes of liquid that can be held in the tubular carbon-filled anode chamber. Such a feature establishes a significant base for air-cathode MFC in practical applications for future wastewater treatment systems. It has also been shown that this system can be operated at high substrate concentrations without recirculation for high power generation. This can greatly decrease the operational costs of the MFC. However, further improvements in technical and economical issues associated with the open-to-air cathode remain necessary to make the GTMFC commercially viable. For example, platinum catalysts used here must be avoided in open-to-air MFCs due to the sensitivity of Pt to poisoning and high catalyst costs. Recently, Zelenay and Bashayam [26] reported a low-cost non-platinum catalyst (Co-PPY-XC72) available for a hydrogen fuel cell and such novel finding may offer an opportunity to use inexpensive and environmentally benign materials in MFCs.

Acknowledgements

This work is supported by Program for Changjiang Scholars and Innovative Research Team in University (PCSIRT), the Ministry of Education, China. The authors would like to sincerely thank Zhibin Zhu and Jie Yu for their technical assistance with EIS analysis and SEM observations, and Dr. Bruce E Logan (Penn. State) for comments and assistance with the manuscript preparation for publication. Dr. Kun Wang is gratefully thanked for her kindest supports during the course of this study.

References

- [1] D.R. Bond, D.R. Lovley, *Appl. Environ. Microbiol.* 69 (2003) 1548–1555.
- [2] H.J. Kim, H.S. Park, M.S. Hyun, I.S. Chang, M. Kim, B.H. Kim, *Enzyme Microbiol. Technol.* 30 (2002) 145–152.
- [3] S.K. Chaudhuri, D.R. Lovley, *Nat. Biotechnol.* 21 (2003) 1229–1232.
- [4] H.S. Park, B.H. Kim, H.S. Kim, H.J. Kim, G.T. Kim, M. Kim, I.S. Chang, Y.K. Park, H.I. Chang, *Anaerobe* 7 (2001) 297–306.
- [5] C.A. Pham, S.J. Jung, N.T. Phung, J. Lee, I.S. Chang, B.H. Kim, H. Yi, J. Chun, *FEMS Microbiol. Lett.* 223 (2003) 129–134.

- [6] K. Rabaey, N. Boon, S.D. Siciliano, M. Verhaege, W. Verstraete, *Appl. Environ. Microbiol.* 70 (2004) 5373–5382.
- [7] G. Reguera, K.D. McCarthy, T. Mehta, J.S. Nicoll, M.T. Tuominen, D.R. Lovley, *Nature* 435 (2005) 1098–1101.
- [8] F. Kaufmann, D.R. Lovley, *J. Bacteriol.* 183 (2001) 4468–4476.
- [9] S.E. Oh, B. Min, B.E. Logan, *Environ. Sci. Technol.* 38 (2004) 4900–4904.
- [10] U. Schroder, J. Nieben, R. Scholz, *Angew. Chem. Int. Ed. Engl.* 42 (2003) 2880–2883.
- [11] K. Rabaey, G. Lissens, S.D. Siciliano, W. Verstraete, *Biotechnol. Lett.* 25 (2003) 1531–1535.
- [12] S.J. You, Q.L. Zhao, J.N. Zhang, J.Q. Jiang, S.Q. Zhao, *J. Power Sources* 162 (2006) 1409–1415.
- [13] H. Liu, B.E. Logan, *Environ. Sci. Technol.* 38 (2004) 4040–4046.
- [14] H. Liu, S. Cheng, B.E. Logan, *Environ. Sci. Technol.* 39 (2005) 658–662.
- [15] H. Liu, S. Cheng, B.E. Logan, *Environ. Sci. Technol.* 39 (2005) 5488–5493.
- [16] S. Cheng, H. Liu, B.E. Logan, *Environ. Sci. Technol.* 40 (2006) 2426–2432.
- [17] B.E. Logan, B. Hamelers, R. Rozendal, U. Schroder, J. Keller, S. Freguia, P. Aelterman, W. Verstraete, K. Rabaey, *Environ. Sci. Technol.* 40 (2006) 5181–5192.
- [18] B.E. Logan, J.M. Regan, *Trends Microbiol.* 14 (2006) 512–518.
- [19] Z. He, N. Wagner, S.D. Minteer, L.T. Angenent, *Environ. Sci. Technol.* 40 (2006) 5212–5217.
- [20] K. Rabaey, P. Clauwaert, P. Aelterman, W. Verstraete, *Environ. Sci. Technol.* 39 (2005) 8077–8082.
- [21] S. Cheng, H. Liu, B.E. Logan, *Electrochem. Commun.* 8 (2006) 489–494.
- [22] D.R. Lovley, E.J.P. Phillips, *Appl. Environ. Microbiol.* 54 (1988) 1472–1480.
- [23] B. Min, S. Cheng, B.E. Logan, *Water Res.* 39 (2005) 1675–1686.
- [24] S. Oh, B.E. Logan, *Appl. Microbiol. Biotechnol.* 70 (2006) 162–169.
- [25] A.R. Konak, *J. Appl. Chem. Biotechnol.* 24 (1974) 453–462.
- [26] P. Zelenay, R. Bashayam, *Nature* 443 (2006) 63.